Materials and Structures (2015) 48:2855–2867
DOI 10.1617/s11527-014-0361-0

ORIGINAL ARTICLE

Experimental study on the lateral behavior of DSCT columns with corrugated inner tube

Taek Hee Han · Deokhee Won · Seungjun Kim · Young Jong Kang

Received: 22 October 2013 / Accepted: 6 June 2014 / Published online: 23 July 2014

Abstract A double-skinned composite tubular column with a corrugated internal tube (DSCT-CT) was suggested to reduce the thickness of the inner tube while maintaining the required buckling strength. The DSCT-CT was studied to evaluate its behavior under lateral loading, and its lateral behavior was compared with that of a DSCT column with a flat internal tube (DSCT-FT). Quasi-static tests were performed by applying cyclic lateral loadings to the two different DSCT columns. Their test results were compared to each other and to those of a solid RC column from other research. The test results showed that the DSCT-CT column had larger ductility than the DSCT-FT column, with an equivalent damping ratio. However, the DSCT-CT column showed a smaller bending moment resistance and energy-absorbing capacity than the DSCT-FT column. Overall, the test results showed that the performances of the DSCT columns were superior to that of the solid RC column in terms of strength, yield energy, ultimate energy, and energy-absorbing capacity. As a result of their superior moment capacities, the DSCT columns absorbed about 50 % more energy than the solid RC column. However, the DSCT columns showed lower energy ductility factors than the solid RC column because of their high yield energies.

Keywords DSCT · Column · Composite · Concrete · Double skinned · Corrugate

List of symbols

$0.75V_{max}$	75 % of the maximum load
$0.8V_{max}$	80 % of the maximum load
D	Outside diameter of confined concrete or inside diameter of outer tube
D_i	Diameter of hollow section or inside diameter of confined concrete
D_o	Outside diameter of the outer tube
E	Modulus of elasticity
e_b	Balanced eccentricity
f_{it}	Stress acting on the inner tube
f_{ity}	Yield strength of the inner tube
f_{bk}	Buckling strength of the inner tube
f_{lim}	Smaller value between yield strength and buckling strength of inner steel tube
f_{oty}	Yield strength of the outer tube
I	Moment of inertia

T. H. Han · D. Won
Coastal Development & Ocean Energy Research Division, Korea Institute of Ocean Science and Technology, Ansan 426-744, Republic of Korea

S. Kim
Coastal & Ocean Engineering Div., Dept. of Zachry Civil Engineering, Texas A&M University, College Station, TX 77840, USA

Y. J. Kang (✉)
School of Department of Architectural, Civil and Environmental Engineering, Korea University, Seoul 156-701, Republic of Korea
e-mail: yjkang@korea.ac.kr

M_0	Nominal moment without axial load
M_b	Nominal moment under balanced condition
t_{eq}	Equivalent thickness of the corrugated tube
t_i	Thickness of the inner tube
t_o	Thickness of the outer tube
t_y	Required minimal thickness of the inner tube to prevent its premature yielding
w_f	Height of the wave
w_l	Length of one-half of a wave
w_s	Arc-length of one-half of a wave
P_0	Nominal axial strength without eccentricity
P_b	Nominal axial strength under balanced condition
P_{DSCT}	Axial strength of a DSCT column
P_{SUM}	Sum of individual axial strengths of the component members of a DSCT column
ν	Poisson's ratio

1 Introduction

Concrete filled tubular (CFT) members have been used in many architectural structures because of their superior performances. However, unlike RC members, they are not commonly used as bridge piers because a typical bridge pier has a large cross-sectional diameter. If it were possible to reduce the cross section and self-weight of a CFT column with no loss in capacity, it could conveniently be used as a bridge pier. Based on this concept, a double-skinned composite tubular (DSCT) column was introduced as shown in Fig. 1 [1]. One steel tube is place inside another, and the space between them is filled with concrete. Since its introduction, numerous researchers have studied the enhanced axial strength of a DSCT column, and the results of many experiments have shown that the axial strength of a DSCT column (P_{DSCT}) is higher than the sum of the individual axial strengths (P_{SUM}) of the component members (the two steel tubes and the concrete between them). Wei et al. [2, 3] showed that the strength of a DSCT member was 10–30 % higher than the sum of the axial strengths of its individual components: the concrete, inner tube, and outer tube. They proposed an empirical formula for the axial strength of a DSCT member. Other researchers have studied the axial strength and ductility of a DSCT column with a square [4] or circular [5] cross section. Recently, Han et al. [6] proposed a nonlinear concrete model for a DSCT column that considered the confining effect by using the unified concrete model suggested by Mander et al. [7]. They argued that the confining effect significantly affected the strength of a DSCT column and that this confining effect generated the strength difference between P_{DSCT} and P_{SUM} seen in the previous studies [2, 3]. Meanwhile, most studies have focused on the axial strength of a DSCT column. Recently, the bending strength of a DSCT column has been studied. Han et al. [8, 9] studied the behavior of DSCT beam-columns under cyclic bending using an experimental method and an analytical method. In their study, DSCT column specimens with circular and square cross sections were tested under cyclic bending. But their diameters were very small (114 and 120 mm) [8]. The test results showed that DSCT columns with circular sections dissipate more energy than DSCT columns with square sections [8]. They proposed an analytical model to predict the behavior of a DSCT column based on other analytical and experimental researches [9]. They showed the behaviors of the moment versus the curvature response and the lateral load versus the lateral displacement. Another study by Han et al. [10] proposed a DSCT column model that considered the confining effect and material nonlinearity. They also proposed a DSCT column with a corrugated internal tube and showed its performance as a beam-column. Moreover, they analytically showed that a DSCT column with a corrugated internal tube (DSCT-CT) has a larger ductility factor than a DSCT column with a flat internal tube (DSCT-FT).

Recently, ocean renewable energies, which are offshore wind power, current power, and tidal current power, have attracted much attention. Therefore, some ocean energy sites have been surveyed [11–13] and several ocean energy power plants such as the Uldolmok tidal current power plant [14] and Shiwha tidal power plant have been built and are being operated in Korea. In addition, because of the superior axial strength and bending resistance capacity of DSCT columns, many engineers are attempting to apply them to various structures such as an offshore wind power tower, the substructures of a tidal current power plant, and the piers for a light-weight railway bridge. Therefore, more research on the various types

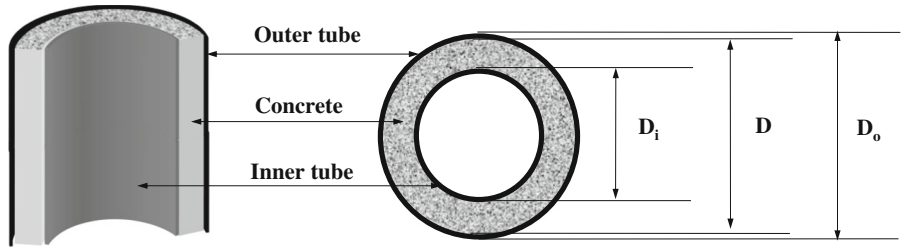

Fig. 1 Cross section of DSCT column

of DSCT columns is required to widen the scope of their application.

In this study, a DSCT column with a corrugated internal tube was proposed, and its lateral behavior was investigated using an experimental method. Two DSCT columns were tested to evaluate their performances under cyclic lateral loading. Quasi-static tests were carried out. The test results were compared to each other and to those for a solid RC column [15].

2 Experiment

Han et al. [6] defined three failure modes for a DSCT column by considering the failure conditions of the inner and outer tubes. They suggested Eq. (1) to determine the failure mode of a DSCT column, with consideration given to the stress conditions. The first failure mode is defined as the inner tube failing by buckling or yielding before the outer tube yields. The reverse condition is the second failure mode. In the second mode, the inner tube does not yield and is not buckled before the outer tube yields. In the third failure mode, the inner and outer tubes fail simultaneously. In the first failure mode, the concrete of the DSCT column is in a triaxially confined state before the inner tube fails. After the inner tube fails, it is assumed to exert no more confining pressure. In the second failure mode, the concrete is completely confined before the DSCT column fails by the yielding or buckling of the outer tube. In the third failure mode, the concrete is also completely confined before the DSCT column fails, but a sudden collapse occurs. Therefore, it is supposed that the optimum performance of a DSCT column will be achieved when the inner tube does not fail before the outer tube yields. The yielding failure criterion of the inner tube determines the limit confining pressure on the concrete by the inner tube. The buckling failure of the inner tube results in a loss of confining pressure.

$$f_{\mathrm{it}} > f_{\mathrm{lim}} = \mathrm{smaller}\left(f_{\mathrm{ity}}, f_{\mathrm{bk}}\right) : \text{Failure Mode 1} \tag{1a}$$

$$f_{\mathrm{it}} < f_{\mathrm{lim}} = \mathrm{smaller}\left(f_{\mathrm{ity}}, f_{\mathrm{bk}}\right) : \text{Failure Mode 2} \tag{1b}$$

$$f_{\mathrm{it}} < f_{\mathrm{lim}} = \mathrm{smaller}\left(f_{\mathrm{ity}}, f_{\mathrm{bk}}\right) : \text{Failure Mode 2} \tag{1c}$$

It is important to design a DSCT column to have failure mode 2, and this can be controlled by the thickness of the inner tube. Han et al. [6] derived Eqs. (2) and (3) to calculate the minimum required thicknesses of the inner tube to prevent its yielding and buckling, respectively, before the outer tube yields. For an inner tube with corrugations, as shown in Fig. 2, they suggested Eq. (9) to estimate its minimum required thickness to prevent buckling failure. A corrugated plate can be analyzed by replacing the thickness of the plate with an equivalent thickness [16]. The flexural rigidity values of a plate for each direction of the x- and y-axes are respectively given by Eqs. (4) and (5) when the corrugation is described as a sine function. The arc-length of one-half of a wave (w_s) and the moment of inertia (I) can be approximately calculated by Eqs. (6) and (7), respectively, using the height of a wave (w_f) [16]. By letting t_{eq} be the equivalent thickness of a flat tube with a buckling strength equal to that of the corrugated tube, Eq. (8) is given and Eq. (9) is derived.

$$t_{\mathrm{y}} = \frac{D_{\mathrm{i}} f_{\mathrm{oty}}}{D \cdot f_{\mathrm{ity}}} t_{\mathrm{o}} \tag{2}$$

$$t_{\mathrm{bk}} = \sqrt{\frac{6}{2.27} \frac{D_{\mathrm{i}}^2 f_{\mathrm{oty}} t_{\mathrm{o}}}{D \cdot E}} \tag{3}$$

$$D_{\mathrm{x}} = \frac{w_{\mathrm{l}}}{w_{\mathrm{s}}} \frac{E \cdot t_{\mathrm{i}}^3}{12(1 - \nu^2)} \tag{4}$$

$$D_{\mathrm{y}} = EI \tag{5}$$

Fig. 2 Corrugated sheet

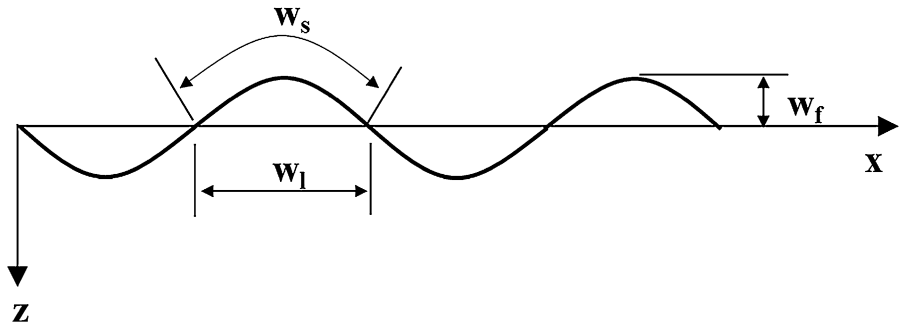

$$w_s = w_l\left(1 + \frac{\pi^2 w_f^2}{4w_l^2}\right) \tag{6}$$

$$I = \frac{w_f^2 \cdot t_i}{2}\left[1 - \frac{0.81}{1 + 2.5\left(\frac{w_f}{2w_l}\right)^2}\right] \tag{7}$$

$$I = \frac{w_f^2 \cdot t_i}{2}\left[1 - \frac{0.81}{1 + 2.5\left(\frac{w_f}{2w_l}\right)^2}\right] = \frac{t_{eq}^3}{12} \tag{8}$$

$$t_{eq} = \sqrt[3]{6w_f^2 \cdot t_i\left[1 - \frac{0.81}{1 + 2.5\left(\frac{w_f}{2w_l}\right)^2}\right]} \tag{9}$$

Based on the theoretical failure modes of a DSCT column [6], two DSCT column specimens were fabricated for experiments. One DSCT column had a flat inner steel tube (DSCT-FT), and the other had a corrugated inner steel tube (DSCT-CT). The two tested columns had equal heights, inner and outer diameters, and outer steel tube thicknesses, but had different thicknesses for their inner steel tubes. The heights from the top of the footing to the top of the column and to the center of the loading face were 2,650 and 2,250 mm, respectively. The height of the footing was 1,000 mm. Quasi-static tests were carried out. The test results for the two different DSCT columns were compared with each other. Because RC columns are most popular for civil structures, the test results were also compared with those of a solid RC column [15], which had equal height to the DSCT column specimens and was tested by same loading history of them. All of the compared columns had equal heights and concrete strengths, and the confined concrete diameters were almost equal.

2.1 Column specimen

The DSCT column specimen was designed to have a confined concrete diameter of 558.8 mm and a hollow section diameter of 406.4 mm. The confined concrete diameter of the DSCT column was determined to be close to that of the referencing solid RC column (594 mm). Figure 3 shows the cross-sectional dimensions of the DSCT columns and the solid RC column for comparison [15]. Two different steel tubes were used for the DSCT column specimens, which were a flat inner steel tube for the DSCT-FT column and a corrugated inner steel tube for the DSCT-CT column. Their material properties are provided in Table 1. The outer tube was made of an SM400 steel plate (ultimate strength = 400 MPa [17]) and was fabricated using rolling and welding work in a factory. The thickness of the outer steel tube was determined by Eq. (10), which was based on the Design Specification for Concrete Structures of Korea [18]. This equation is a guide for the steel tube of a CFT column, and it provides the required minimum thickness for the outer tube to avoid local buckling failure by axial loading. The minimum thickness of the outer tube was calculated to be 8.95 mm using Eq. (10), and the design thickness was determined to be 10 mm, which was the smallest thickness for a factory product satisfying Eq. (10).

$$t_o > (D_o + t_o)\sqrt{\frac{f_{oty}}{8E}} \tag{10}$$

An electrically welded steel tube pile (ERW, KSF 4602 [17]) was used as the flat inner steel tube because it had the most appropriate diameter from among available factory-products for the planned hollow ratio, which was about 0.7. Its outer diameter and thickness were 406.4 and 9 mm, respectively. Its

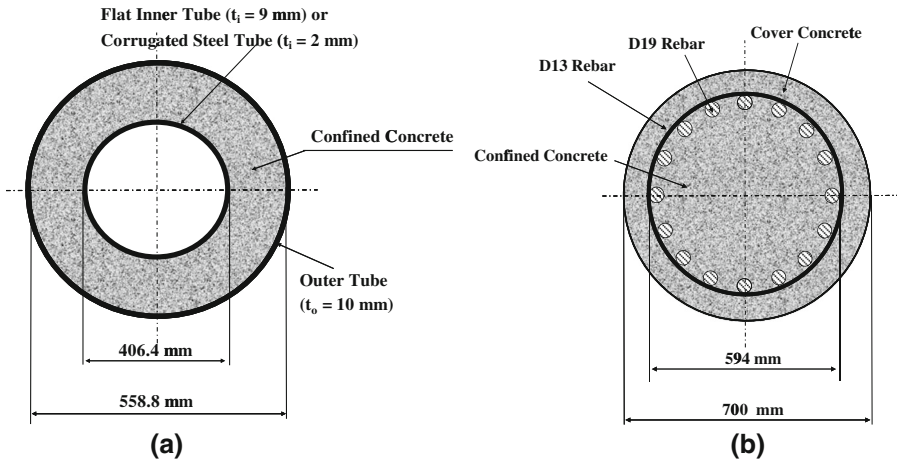

Fig. 3 Cross-sectional dimensions of designed columns: **a** DSCT column and **b** solid RC column

Table 1 Material properties

Component	Yield strength (MPa)*	Ultimate strength (MPa)*	Modulus of elasticity (MPa)**	Ultimate strain**
Flat inner steel tube	378.2	588.6	206,010	0.16
Corrugated inner steel tube	206.0	274.1	206,010	0.16
Outer steel tube	250.0	400.0	206,010	0.16

* Provided from manufacturer's material test. ** Manufacturer's recommendation

required minimum thicknesses to prevent yielding and buckling were 5.54 and 3.02 mm, respectively. Therefore, the DSCT-FT column specimen was expected to have failure mode 2, which was the case where the outer steel tube would fail before the inner steel tube. A corrugated inner steel tube with a diameter equal to that of the flat inner steel tube was selected for the DSCT-CT column specimen. Its outer diameter was 406.4 mm. Its thickness (t_i), height of the wave (w_f), and length of one half of a wave (w_l) were 2, 6.5, and 34 mm, respectively. Its required minimum thicknesses to prevent yielding and buckling were 8.47 and 0.13 mm, respectively. Because its yield strength was lower than that of the flat inner steel tube, its required minimum thickness to prevent yielding was found to be much larger than that of the flat tube. However, its required minimum thickness to prevent buckling was found to be smaller than that of the flat inner steel tube. Because the corrugated inner steel tube had a smaller thickness than its required minimum thickness (8.74 mm), the DSCT-CT column specimen was expected to have failure mode 1, which was the case where the inner steel tube would fail before the outer steel tube.

From 28-day tests of three cylindrical molds, the compressive strength of the concrete was found to be 21.72 MPa by averaging the measured strengths of 21.66, 21.23, and 22.28 MPa. To join the inner tube and concrete, eight shear connectors were welded around the outer surface of the inner steel tube in the circumferential direction, with a spacing of 200 mm between sets of connectors in the longitudinal direction, as shown in Fig. 4. The designed shear connector had a cross-shaped section to play the roles of a shear connector for the composition and a stiffener to prevent the local buckling of the inner tube. It was designed to have an equal cross-sectional area and height to those of a general shear connector currently being used in Korea [18]. The spacing was determined to resist the expected shear force based on the analysis result. The cross-shaped shear connector was designed to have sufficient length as a stiffener to prevent the local buckling of the inner steel tube. After the test, the specimens were dismantled and its buckling prevention was observed. Figure 5 shows the column specimens under construction. The bottom side of the inner steel tube was welded onto a steel plate, and the outer steel tube was set concentrically around the inner steel

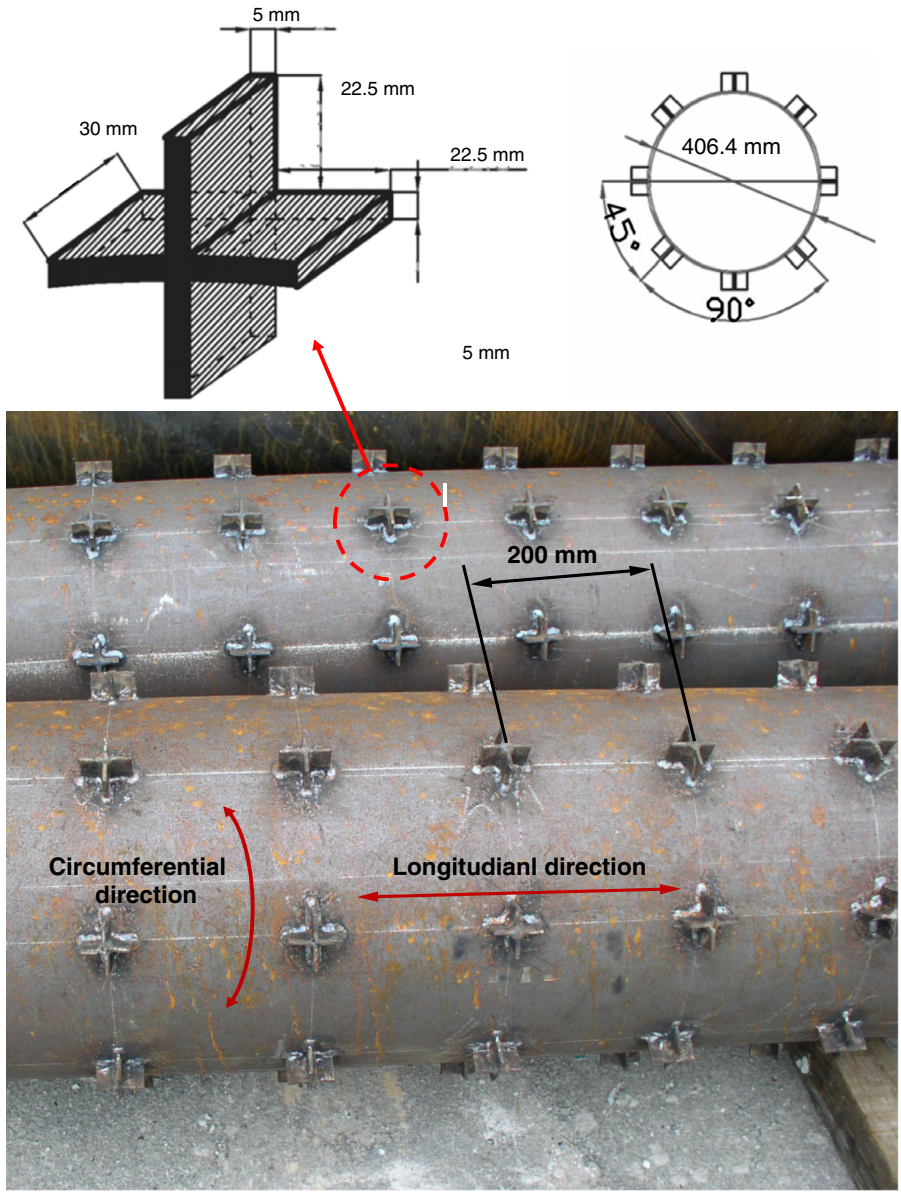

Fig. 4 Shear connectors on inner tubes

tube using spacers. The flat inner steel tube had shear connectors, while the corrugated inner steel tube did not.

2.2 Experimental program

Quasi-static tests were performed using the test setup illustrated in Fig. 6. A cyclic load was applied via a 2,000-kN hydraulic actuator in a displacement-control manner using the planned drift ratios, which were increased by 0.5 % at a time, as shown in Fig. 7. The test was performed until the column specimen lost its stiffness by the rupture of its outer tube. Therefore, the DSCT-CT column specimen was loaded until its outer tube tore horizontally at its plastic hinge as shown in Fig. 8. The DSCT-FT column specimen was observed to lose its stiffness by its increasing displacement although is lateral force decreased. Therefore, DSCT-FT column specimen was loaded until the actuator reached its stroke limit. The loading speed was 5 min

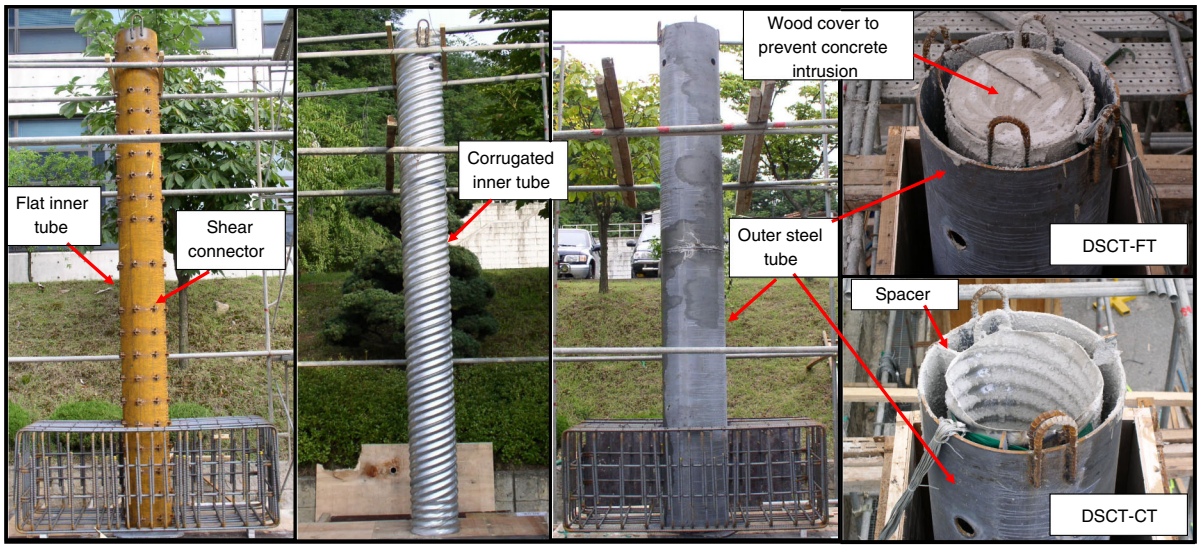

Fig. 5 DSCT column specimens under construction

Fig. 6 Test setup

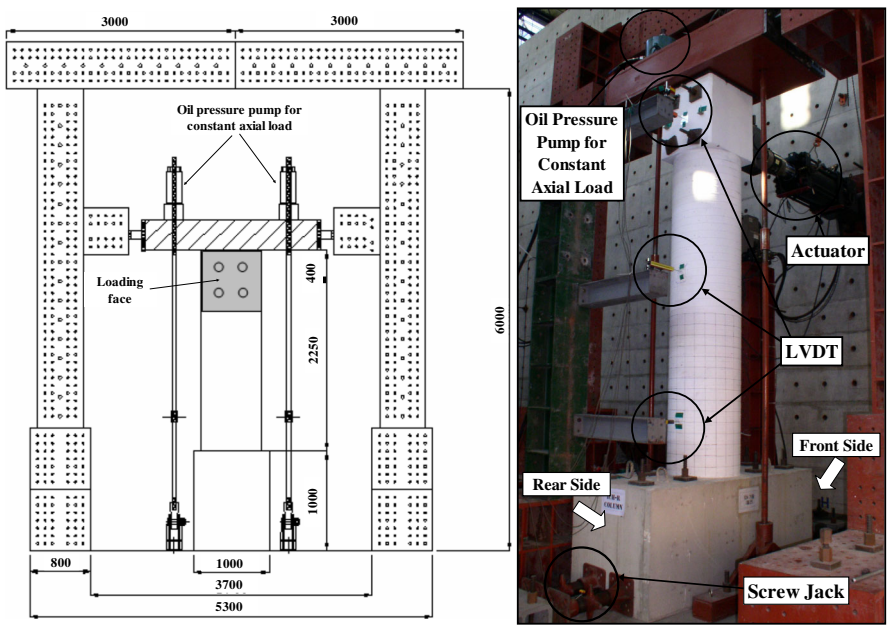

per loading cycle. Using three linear variable differential transducers (LVDTs), the deflections of the column were monitored at heights of 500, 1,300, and 2,250 mm from the top of the footing. At a height of 2,250 mm, which was the loading point, two additional wire gauges were installed to monitor the column specimen and prevent it from twisting. To prevent the footing from sliding, four screw jacks were installed on the front and rear sides of the footing, as shown in Fig. 6. Two LVDTs were also installed to monitor the sliding of the footing. A data logger recorded and stored the test data for each displacement increment at a frequency of one reading per 5 s.

Before the test, the axial force-bending moment interaction was analyzed for the DSCT column specimens with consideration given to the confining effect by CoWiTA [19], which is a nonlinear analysis tool with the consideration of the confining effect of

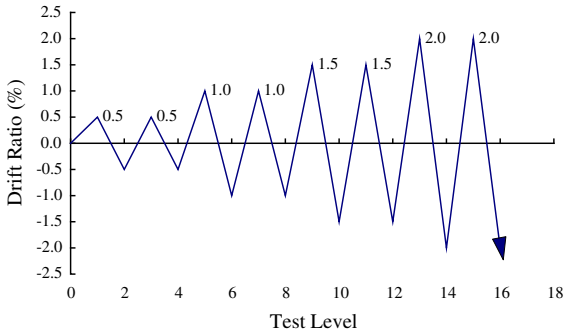

Fig. 7 Loading history

concrete and material nonlinearities based on the research results by Han et al. [6, 10, 15, 20, 21]. From the analysis, the peak axial strengths for the DSCT-FT and DSCT-CT columns were expected to be 15.677 and 6.840 MN, respectively. Based on the analysis results, axial loads of 1,567 and 684 kN, which represented 10 % of the maximum axial strengths, were applied to the DSCT-FT and DSCT-CT columns, respectively. The predicted axial strengths and bending moment resistances are summarized in Table 2.

3 Test results and discussion

In the loading stages, it was observed that the bottom part of the outer steel tube, which was the compression zone of the DSCT column, became inflated, as shown in Fig. 8. By the cyclic loading, the compressed zone alternated with the tensile zone. This alternation gradually tore the outer steel tube of the DSCT-CT column specimen, and it eventually terminated the

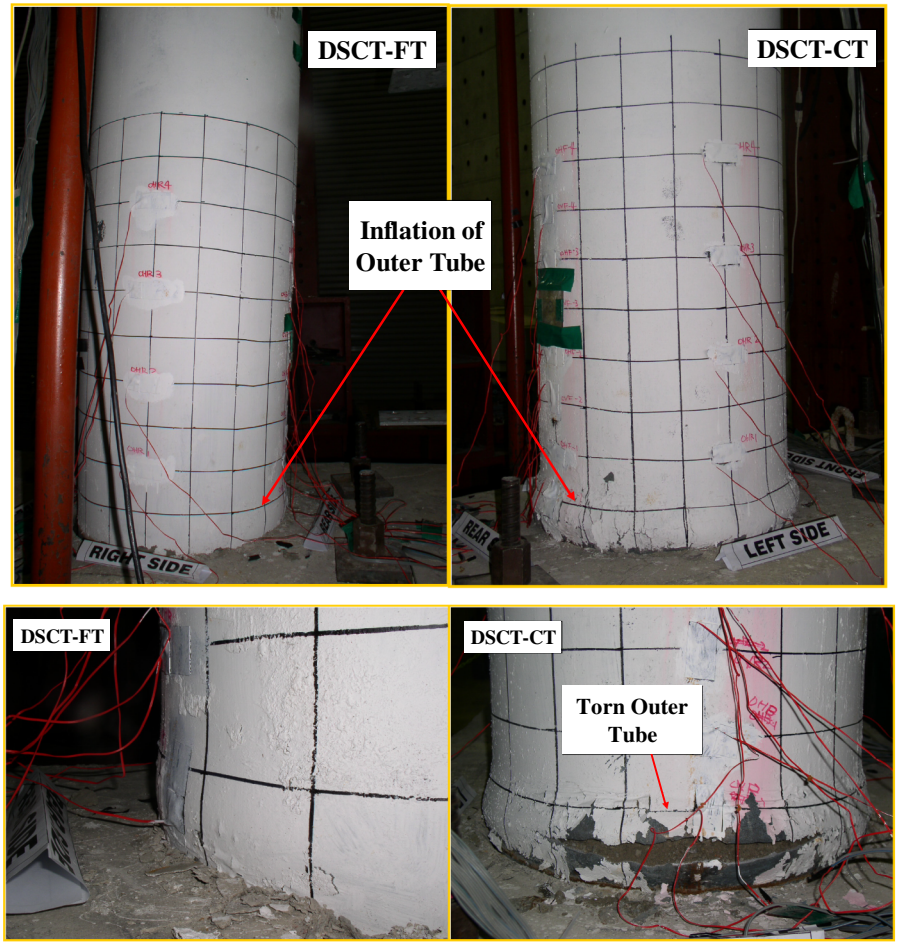

Fig. 8 Inflated and torn outer tube

Table 2 Expected axial strength and bending moment

Specimen	P_0 (kN)	M_0 (kN-m)	P_b (kN)	M_b (kN-m)	e_b (mm)
DSCT-FT	15,677.24	1,805.79	2,623.67	1,887.99	719.60
DSCT-CT	6,840.24	1,058.90	399.76	1,063.32	2,659.92

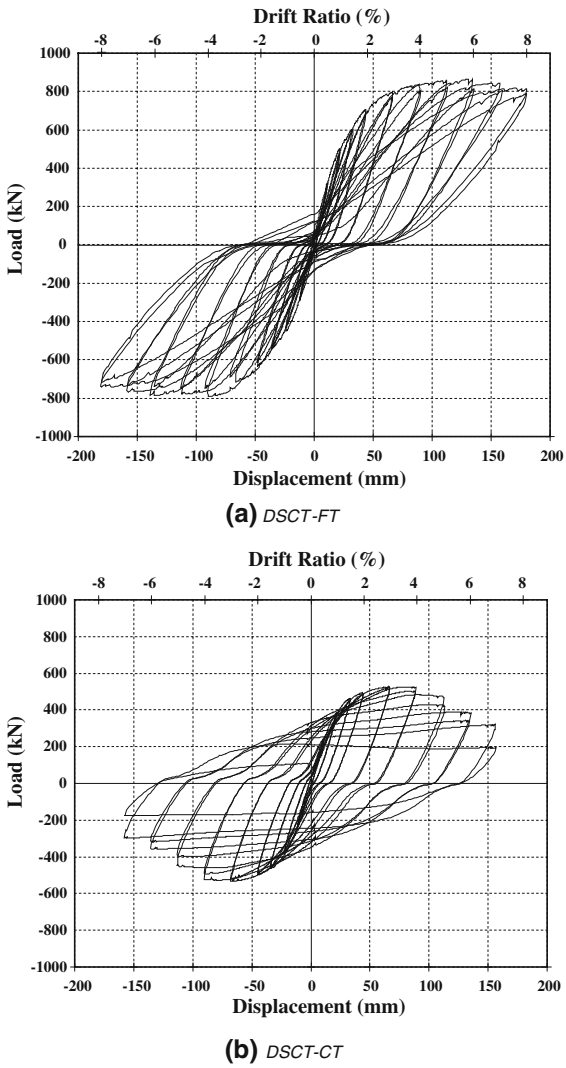

Fig. 9 Hysteresis loops

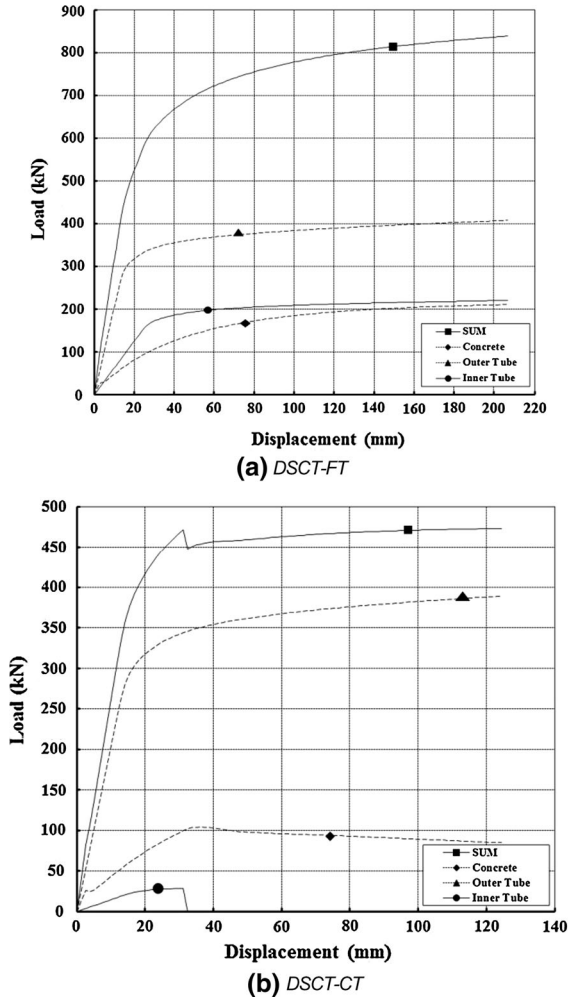

Fig. 10 Strength contribution of component [10]

test. This termination occurred at a drift ratio of 7 % by the rupture of the outer steel tube, as shown in Fig. 8. Pulverized concrete was observed through the torn and open outer steel tube. Unlike the DSCT-CT column specimen, the test of the DSCT-FT column specimen was manually terminated at a drift ratio of 8 % before its rupture, because of the insufficient stroke of the actuator. Therefore, no tear in the outer steel tube was observed in this test.

The load–displacement hysteresis loops of the DSCT-FT and DSCT-CT column specimens were acquired from the test results, as shown in Fig. 9. The maximum applied loads on the DSCT-FT column and DSCT-CT column were 801.10 and 523.63 kN,

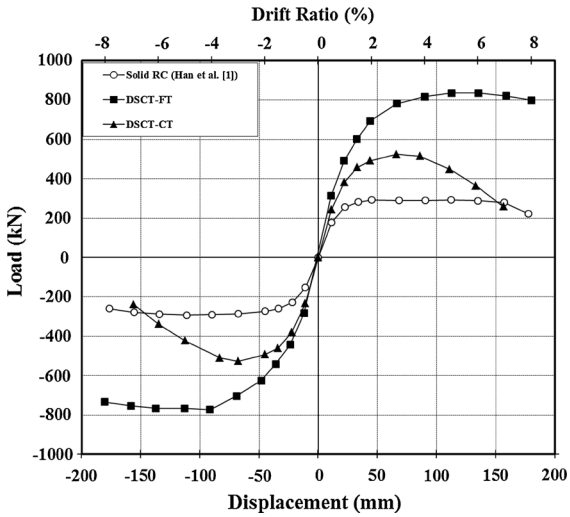

Fig. 11 Envelope curves

respectively. Therefore, their maximum bending moments were 1,822.72 kN-m (DSCT-FT) and 1,178.17 kN-m (DSCT-CT). As shown in Fig. 9, they show significant differences in terms of stiffness and maximum load by their different failure modes. Before the test, the DSCT-FT and DSCT-CT columns were expected to have the failure mode 2 and 1, respectively. Figure 10 shows strength contribution of each component in DSCT columns and little contribution of the inner tube in the DSCT-CT column by its premature failure. As shown in Table 2, the predicted balanced moments were 1,887.99 and 1,063,32 kN-m for DSCT-FT and DSCT-CT columns, respectively. The ultimate displacements for the DSCT-FT and DSCT-CT columns were 180.38 and 119.00 mm, respectively. The yield displacements and ultimate displacements from the experimental results were calculated using the method suggested by Park [22]. He defined the yield displacement and ultimate displacement as the displacements corresponding to 75 and 80 % of the maximum load ($0.75V_{max}$ and $0.8V_{max}$), respectively. If the final load is larger than $0.8V_{max}$, the final displacement is taken as the ultimate displacement.

In Fig. 11, the lateral load-lateral displacement envelope curves of the DSCT column specimens are plotted from the hysteresis loops. In addition, the envelope curve of the solid RC column [15] is also provided for comparison in Fig. 11. The maximum loads, maximum moments, yield displacements, ultimate displacements, yield energies, ultimate energies, displacement ductility factors, and energy ductility factors of the DSCT columns and the solid RC column are summarized in Table 3. As can be seen in Table 3, the DSCT-FT and DSCT-CT columns showed much higher bending strengths than the solid RC column—by 171.7 and 77.6 %, respectively. The DSCT-FT column showed the largest moment resisting capacity (1,802.48 kN-m). The maximum bending moment of the DSCT-CT column was 1,178.27 kN-m. This result indicates that the inner corrugated steel tube contributed little to the moment-resisting capacity because of its small thickness and the accordion effect of its corrugation. Therefore, the thin corrugated inner steel tube contributed only to the confinement of the concrete. However, the outer steel tube of the DSCT-CT column contributed greatly to the moment-resisting capacity. Therefore, the DSCT-CT column showed a much higher strength than the solid RC.

Table 3 shows that the DSCT-FT column had the largest yield and ultimate displacements. It had almost double (196.2 %) the yield displacement of the solid RC column, while its ultimate displacement was almost equal (102.0 %) to that of the solid RC column. The DSCT-CT column had a larger yield displacement (123.1 %) but a smaller ultimate displacement (67.3 %) than the solid RC column. For these reasons, the displacement ductility factors of the DSCT-FT and DSCT-CT columns were almost half that of the solid RC column, although they had much higher bending strengths than the solid RC column. The high yield strength of the DSCT column resulted in a large yield displacement, which could explain why the DSCT column specimens had smaller ductility factors than the solid RC column specimen. However, the displacement ductility factors of the DSCT-FT and DSCT-CT columns were 3.54 and 3.72, respectively. These were much smaller than that of the solid RC column (6.80).

The yield energies of the solid RC, DSCT-FT, and DSCT-CT column specimens were calculated to be 4.11, 22.58, and 8.46 kN-m, respectively. The ultimate energies were 47.10, 123.25, and 51.39 kN-m for the solid RC, DSCT-FT, and DSCT-CT column specimens, respectively. The energy ductility factors for the column specimens showed the same trend as the displacement ductility factors. However, they were larger than the corresponding displacement ductility factors. The energy ductility factors for the DSCT-FT

Table 3 Maximum load and ductility factor

Column type	Solid RC (Han et al. [1])		DSCT-FT		DSCT-CT	
Maximum load (kN)	294.83	100.0 %	801.10	271.7 %	523.63	177.6 %
Maximum moment (kN-m)	663.37	100.0 %	1802.48	271.7 %	1178.17	177.6 %
Ultimate displacement (mm)	176.78	100.0 %	180.38	102.0 %	119.00	67.3 %
Yield displacement (mm)	26.00	100.0 %	51.00	196.2 %	32.00	123.1 %
Ultimate energy (kN-m)	47.10	100.0 %	123.25	261.7 %	51.39	109.1 %
Yield energy (kN-m)	4.11	100.0 %	22.58	548.9 %	8.46	205.7 %
Displacement ductility factor	6.80	100.0 %	3.54	52.0 %	3.72	54.7 %
Energy ductility factor	11.45	100.0 %	5.46	47.7 %	6.07	53.0 %

Table 4 Calculated energy

Calculated energy (kN-m)	Column type	Drift ratio (%)									
		0.5	1.0	1.5	2.0	3.0	4.0	5.0	6.0	7.0	8.0
Input energy	Solid RC [1]	4.42	12.58	22.78	32.81	58.76	84.00	110.03	138.09	161.63	155.02
	DSCT-FT	7.61	23.17	43.28	65.87	116.99	172.80	223.84	245.10	323.25	367.33
	DSCT-CT	5.89	19.23	38.72	62.63	124.41	186.41	234.93	243.02	205.30	–
Cumulative input energy	Solid RC [1]	4.42	17.00	39.77	72.59	131.35	215.35	325.38	463.47	625.10	780.12
	DSCT-FT	7.61	30.77	74.05	139.92	256.91	429.71	653.55	898.64	1221.89	1589.23
	DSCT-CT	5.89	25.12	63.85	126.48	250.88	437.30	672.22	915.24	1120.54	
Absorbed energy per cycle	Solid RC [1]	1.56	4.70	11.06	19.00	43.01	67.00	91.89	118.89	142.35	138.35
	DSCT-FT	2.12	7.61	16.84	28.48	61.37	98.15	134.52	150.15	197.32	228.22
	DSCT-CT	1.48	6.42	19.64	39.83	97.17	158.01	212.09	225.50	193.74	–
Cumulative absorbed energy	Solid RC [1]	1.56	6.26	17.32	36.32	79.33	146.32	238.21	357.10	499.45	637.80
	DSCT-FT	2.12	9.73	26.57	55.05	116.41	214.56	349.08	499.23	696.55	924.78
	DSCT-CT	1.48	7.89	27.54	67.37	164.54	322.55	534.64	760.14	953.87	–
Elastic strain energy	Solid RC [1]	3.69	10.57	18.37	25.41	39.03	52.73	65.00	77.54	87.18	90.86
	DSCT-FT	6.80	21.25	39.11	60.59	100.59	144.38	180.75	218.13	249.74	276.42
	DSCT-CT	5.23	16.93	30.69	43.69	70.38	86.58	97.32	94.21	77.58	–

and DSCT-CT columns were 5.46 and 6.07, respectively. These were smaller than that of the solid RC (11.45) column specimen. The acquired results showed that the DSCT columns had lower energy ductility values than the solid RC column, although they had much higher strengths and ultimate energies. This resulted from their larger yield displacements and higher yield energies than those of the solid RC column. It is supposed that if the thickness of the outer tube decreases, the ductility factor of a DSCT column will increase. However, this would make its strength lower. If a DSCT column has a smaller diameter but a bending strength equal to that of a solid RC column, its ductility factor will increase, as argued by Han et al. [6]. The energies at the drift ratios for the column specimens are summarized in Table 4. This information could be used to calculate the absorbed energies of the column specimens, as shown in Fig. 12.

Figure 11 shows the energy-absorbing capacities of the DSCT columns and the solid RC column from the

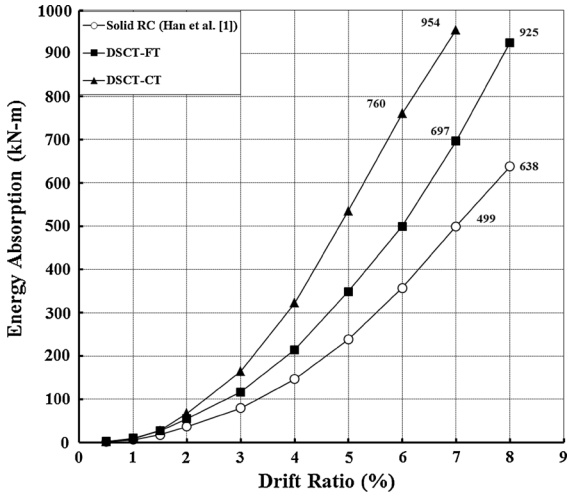

Fig. 12 Energy absorption

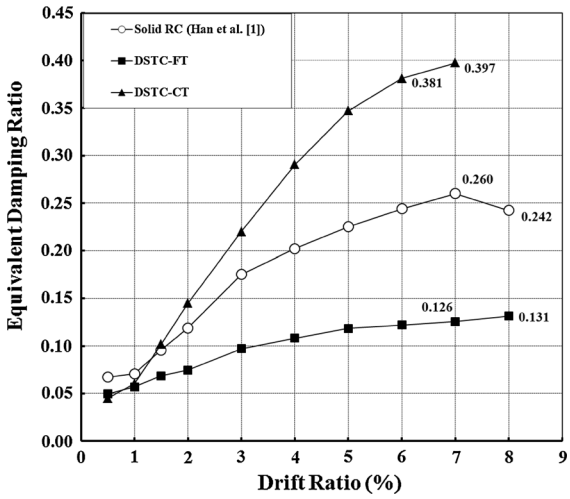

Fig. 13 Equivalent damping ratio

hysteresis loops. At the final drift ratio, the absorbed energies were 638, 925, and 954 kN-m for the solid RC, DSCT-FT, and DSCT-CT columns, respectively. These results show that the DSCT column specimens absorbed 45 % more energy than did the solid RC column specimen. Figure 13 shows the equivalent damping ratios for the tested specimens based on the method suggested by Loh et al. [23]. At the final drift ratio, the DSCT-CT column specimen showed a larger equivalent damping ratio (0.397) than the solid RC column specimen (0.242). However, the DSCT-FT column specimen showed the smallest equivalent damping ratio (0.131).

4 Conclusions

The following conclusions were drawn based on the experimental results, and it was experimentally verified that a DSCT column has superior moment-resisting capacity to a solid RC column.

1. The DSCT columns had superior bending moment resistances to a solid RC column with an equal outer diameter. The DSCT-FT and DSCT-CT columns respectively showed bending moment capacities of 271.7 and 177.6 % relative to the solid RC column. The moment capacity of a DSCT column could be enhanced by increasing the thickness of its outer tube without enlarging the outer diameter of the column.
2. The DSCT columns showed much smaller ductility factors than the solid RC column. Their displacement ductility factors were 52.0–54.7 % compared to that of the solid RC column. In addition, their energy ductility factors were 48.2–53.5 % compared to that of the solid RC column. These resulted from their high yield strength and small yield displacement, even though they had superior moment-resisting capacities.
3. Because of their superior moment-resisting capacities, the DSCT columns absorbed much more energy than did the solid RC column. At the drift ratio of 7 %, the DSCT-CT column absorbed almost double the energy (191 %) of the solid RC column. At the drift ratio of 8 %, the DSCT-FT column absorbed 45 % more energy than the solid RC column.
4. The DSCT-FT column showed a smaller equivalent damping ratio than the solid RC column, but the DSCT-CT column showed a larger equivalent damping ratio than the solid RC column.

Acknowledgments This research was financially supported by the Ministry of Land, Infrastructure and Transport (MOLIT) of the Korea government (code 12 Technology Innovation E09) and Korea Institute of Ocean Science & Technology (Project No. PE99274).

References

1. Shakir-Khalil H, Illouli S (1987) Composite columns of concentric steel tubes. In: Proceeding of Conference on the

Design and Construction of Non-Conventional Structures, pp 73–82
2. Wei S, Mau ST, Vipulanandan C, Mantrala SK (1995) Performance of new sandwich tube under axial loading: experiment. J Struct Eng 121:1806–1814
3. Wei S, Mau ST, Vipulanandan C, Mantrala SK (1995) Performance of new sandwich tube under axial loading: analysis. J Struct Eng 121:1815–1821
4. Zhao X-L, Grzebieta R (2002) Strength and ductility of concrete filled double skin (SHS inner and SHS outer) tubes. Thin Walled Struct 40:199–213
5. Tao Z, Han L-H, Zhao X-L (2004) Behavior of concrete-filled double skin (CHS inner and CHS outer) steel tubular stub columns and beam columns. J Constr Steel Res 60:1129–1158
6. Han TH, Stallings JM, Kang YJ (2010) Nonlinear concrete model for double-skinned composite tubular columns. Constr Build Mater 24(12):2542–2553
7. Mander JB, Priestley MJN, Park R (1988) Theoretical stress–strain model for confined concrete. J Struct Div ASCE 114(8):1804–1826
8. Han LH, Huang H, Tao Z, Zhao XL (2006) Concrete-filled double skin steel tubular (CFDST) beam-columns subjected to cyclic bending. Eng Struct 28:1698–1714
9. Han LH, Huang H, Zhao XL (2009) Analytical behaviour of concrete-filled double skin steel tubular (CFDST) beam-columns under cyclic loading. Thin Walled Struct 47:668–680
10. Han TH, Won DH, Kim S, Kang YJ (2013) Performance of a double-skinned composite tubular column under lateral loading: analysis. Mag Concr Res 65(2):121–135
11. Ro YJ (2007) Tidal and sub-tidal current characteristics in the Kangjin bay, South Sea, Korea. Ocean Sci J 42(1):19–30
12. Rho JY, Jun WS, Jung KY, Eom HM (2007) Numerical modeling of tidal current in the Kangjin Bay, South Sea, Korea. Ocean Sci J 2(3):153–163
13. Lee HJ (2010) Preliminary results on suspended sediment transport by tidal currents in Gomso bay, Korea. Ocean Sci J 45(3):187–195
14. Kang SK, Jung KT, Yum K-D, Lee K-S, Park J-S, Kim EJ (2012) Tidal dynamics in the strong tidal current environment of the Uldolmok waterway, Southwestern tip off the Korean peninsula. Ocean Sci J 47(4):453–463
15. Han TH, Stallings JM, Cho SK, Kang YJ (2010) Behaviour of a hollow RC column with an internal tube. Mag Conc Res 62(1):25–38
16. Timoshenko SP, Woinowsky-Krieger S (1959) Theory of plates and shells. McGraw-Hill Inc, Singapore
17. Ministry of Construction and Traffic (2003) Design specifications for steel structures. Korea Society of Steel Structures, Korea
18. Korea Concrete Institute (2007) Design specifications for concrete structures. Korea Concrete Institute, Korea
19. Han TH (2013) CoWiTA manual. Korea Institute of Ocean Science and Technology, Korea
20. Han TH, Lim NH, Han SY, Park JS, Kang YJ (2008) Nonlinear concrete model for an internally confined hollow reinforced concrete column. Mag Concr Res 60(6):429–440
21. Han TH, Yoon KY, Kang YJ (2010) Compressive strength of circular hollow reinforced concrete confined by an internal steel tube. Constr Build Mater 24(9):1690–1699
22. Park R (1988) Ductility evaluation from laboratory and analytical testing. In: Proceeding of ninth world conference on earthquake engineering, vol 8. Tokyo, Japan, pp 605–616
23. Loh CH, Jean WY, Penzien J (1994) Uniform-hazard response spectra-an alternative approach. Earthq Eng Struct Dyn 23(4):433–445